Ocean Engineering 223 (2021) 108639

Contents lists available at ScienceDirect

Ocean Engineering

journal homepage: www.elsevier.com/locate/oceaneng

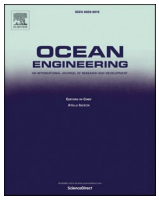

Characteristic current flow through a stocked conical sea-cage with permeable lice shielding skirt

Kristbjörg Edda Jónsdóttir [a,*], Pascal Klebert [b], Zsolt Volent [b], Jo Arve Alfredsen [a]

[a] Norwegian University of Science and Technology, Department of Engineering Cybernetics, NO-7491, Trondheim, Norway
[b] SINTEF Ocean, NO-7465, Trondheim, Norway

ARTICLE INFO

Keywords:
Conical sea cage
Current flow
Atlantic salmon
Permeable lice shielding skirt

ABSTRACT

The characteristic current flow field around a 55 m deep full-scale stocked conical Atlantic salmon sea-cage equipped with a 10 m permeable skirt was studied experimentally using acoustic Doppler velocimeters and profilers. The weakest current speed was inside the cage at 6 m depth and the highest reduction downstream was recorded behind the shielded volume. Downstream of the cage the reduction in speed became little to non-existing at 22 m depth, probably due to the decreasing diameter of the cage with depth. To reduction in current speed through the cage was compared with estimated reduction from theoretical expressions. The results compared reasonably well downstream of the shielded cage, while the reduction inside the cage was higher than the estimates. The difference in current flow field behind a conical cage compared with a cylindrical cage may have implications for the dispersal of waste, feed pellets and microorganisms from the cage influencing the benthic impact of the farm.

1. Introduction

The flow field characteristics around and through a sea cage govern the distribution of feed, waste and dissolved oxygen in the cage, and the sedimentation process that occurs under and behind the cage. How the current flows through and around fish cages is determined by the farm layout (Rasmussen et al., 2015), local topography, flow conditions at the site (Klebert et al., 2013), biomass within the cage (Klebert et al., 2013; Gansel et al., 2014; Klebert and Su, 2020) and the cage structure itself (Klebert et al., 2015). Most cages used in Norway are of the "gravity" type cages, which have a surface collar structure from which a net is suspended. These nets are often weighed down by a sinker ring, resulting in the net having a cylindrical shape above this ring, and a conical shape beneath it.

As the current passes through the net a reduction in current speed occurs (see for example: Løland 1993; Patursson 2008; Klebert et al., 2013). The reduction in current speed in combination with turbulence induced by the net structure has a direct impact on the dispersal of particle and micro-organisms such as pathogens and zooplankton (Klebert and Su, 2020). The reduction in speed increases with solidity which can be due to biofouling (Bi et al., 2013; Gansel et al., 2015), biomass in cage (Klebert and Su, 2020) or increasing inclination angle between the net and vertical direction (Bi et al., 2013; Zhao et al., 2015). This increase in inclination angle can be caused by the cage deformation, as when exposed to strong currents the cage wall upstream and downstream are deformed, and the bottom net is lifted upwards (Fredheim, 2005; Lader et al., 2008; Lien et al., 2014; Klebert et al., 2015).

The reduction in current speed is further enhanced with the use of lice shielding skirts (Frank et al., 2015). The high cost of delousing treatments (Abolofia et al., 2017; Iversen et al., 2017) has led to an increased use of lice shielding skirts as a preventative measure against the salmon lice. Shielding skirts attempt to reroute the upper water column around the cage which has a higher lice density than the deeper levels (i.e. Huse and Holm 1993; Heuch et al., 1995; Hevrøy et al., 2003; Oppedal et al., 2017; Geitung et al., 2019). These skirts are usually made of tarpaulin, which block the current, and some sites experience low DO levels when using such skirts (Stien et al., 2012), which reduces feed intake and specific growth rates (Remen et al., 2014). To counter this, permeable skirts have been introduced. Results from sites applying permeable skirts indicate good DO levels, with a minimum value of 70% DO over a 3-month period (Stien et al., 2018) and no impact on welfare status of the salmon (Bui et al., 2020).

The current flow through normal gravity cages, both with and without skirts, have been studied both through experimental work and

* Corresponding author.
E-mail addresses: kristbjorg.jonsdottir@ntnu.no, kristbjorg.jonsdottir@sintef.no (K.E. Jónsdóttir).

https://doi.org/10.1016/j.oceaneng.2021.108639
Received 1 October 2020; Received in revised form 12 January 2021; Accepted 13 January 2021

simulations (i.e. Bi et al., 2013; Zhao et al., 2015; Klebert et al., 2013). However, in recent years there has been an increasing prevalence of conical nets (written communication Dybing, Egersund group, 08.09.2020). Little documentation has been obtained on the current flow around these nets so far, but it is necessary to study the current flow characteristics around these cages to understand the farm's biological footprint, and to ensure that good water quality and fish welfare is maintained. The same holds valid for cages which are equipped with permeable skirts. Therefore, in this study, the current flow field around and through a conical full-scale commercial salmon cage equipped with a permeable shield was studied. Current speed and direction were measured both upstream, downstream and inside the cage. The reduction in current speed from upstream to inside, and from upstream to downstream were also compared with expected reduction when using analytical expressions developed for plane nets.

2. Material and methods

2.1. Site description

The measurement campaign was performed 2–5 July 2019 at Fornes farm owned and operated by Nordlaks Oppdrett AS located in Øksfjorden, Lofoten islands, Norway (68°24′35.5″N, 15°25′44.8″E, Fig. 1), and is placed in a fjord which has a narrow strait to the North leading into a larger basin with depths up to 104 m. The farm consists of nine cages arranged in a single row from West to East, and spans an area with a depth of 100 m. Data were collected from the third westernmost cage, with stocked cages at either sides of the cage.

All cages at Fornes had a circumference of 160 m and were equipped with conical nets (Fig. 1). The net had a solidity of 0.16 and was 55 m deep with a concrete weight of 2.4 tonnes in water attached to the tip of the cone. The shielding skirt applied was a permeable canvas lice skirt (Norwegian Weather Protection, Frekhaug, Norway) with a solidity of 51%, mesh opening of 350 × 350 μm and a depth of 10 m. The skirt was weighted with 2 kg/m lead rope at the bottom and installed as a cylinder around the conical net roughly 10 days prior to measurements were carried out. The skirt is one piece of fabric installed with a 10 m overlap. The biomass in the cage during the experiment was 750 tonnes, with 191 310 fish with an average weight of 3.8 kg.

2.2. Equipment description: ADV and DCP

Current speed and direction outside the cage were recorded using two current profilers attached to anchoring buoys on both sides of the cage, pointing downwards with a vertical resolution (cell size) of 1 m. To the South-West of the cage, in position B (Fig. 1), an Aanderaa SeaGuard II Doppler current profiler (DCP) measured continuously with a sampling frequency of 0.5 Hz. The DCP had a velocity accuracy of 0.3 cm/s or ±1% of reading, with a velocity resolution of 0.1 cm/s. The data were averaged and stored every minute. To the North-East of the cage, in position A (Fig. 1), a Nortek Aquadopp current profiler 400 MHz (ADCP) was used. The ADCP had a velocity accuracy of ±0.5 cm/s or ±1% of measured value, and a horizontal and vertical velocity precision of 0.7 cm/s and 2.2 cm/s, respectively. The data were averaged over every 3rd minute. As buoy mounted DCPs can experience bias (Mayer et al., 2007), the first depth cell was excluded from the data set.

Inside the cage the current velocity was measured using Nortek Vector Acoustic Doppler Velocimeters (ADV) with a sampling rate of 8 Hz, with 120 samples per burst and a burst interval of 60 s. The sampling volume was 0.18 cm^3 placed 0.15 m from the probes, and the sensor had an accuracy ±0.5% of measured value ±1 mm/s, velocity precision typical 1% of velocity range (at 16 Hz). The ADVs were suspended from a buoy at 3, 6, 9 and 12 m depths and placed in the centre of the cage, position C in Fig. 1. Given the depth of the site it is assumed that the influence from bathymetry on the measured current speed is negligible.

2.3. Flow velocity reduction

Different studies have been conducted regarding the velocity reduction behind net panels (reviewed in Klebert et al., 2013) in model cages (Kristiansen and Faltinsen, 2015) or numerically (Lee et al., 2008; Bi et al., 2014; Kim et al., 2014). Only a few are performed at full scale in commercial cage with fish (Johansson et al., 2007; Klebert et al., 2015; Klebert and Su, 2020); the latest being conducted in circular cages with or with skirt. In this study, a more complex conical cage geometry is investigated. With a twine thickness (d) of 2.7 mm and a mesh size (s) of

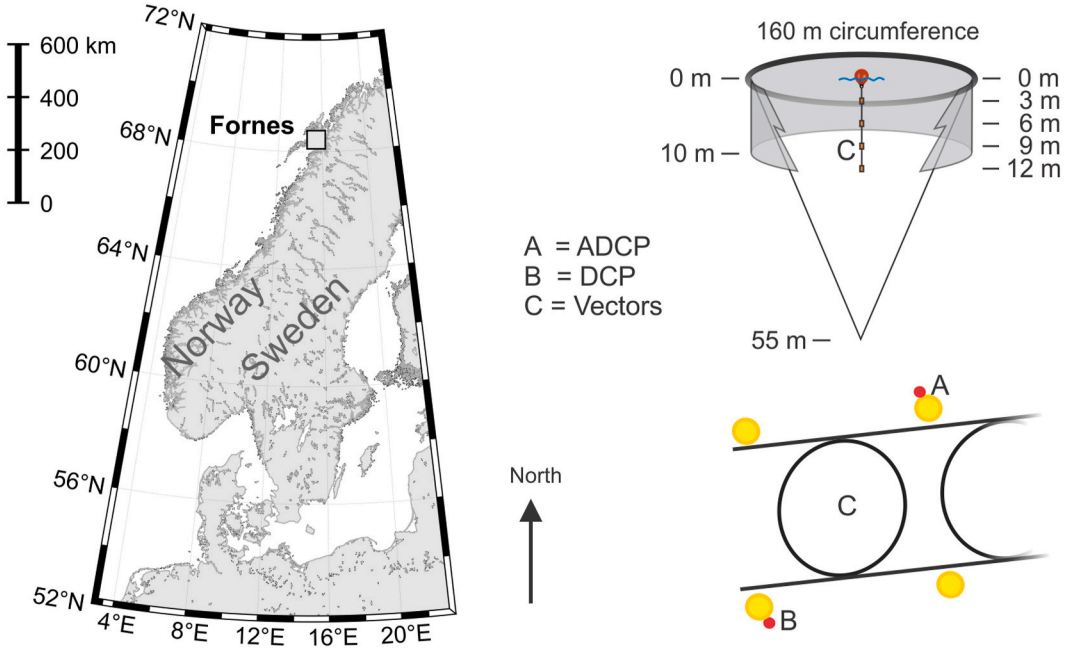

Fig. 1. Left: Location of the fish farm at Fornes were the measurements were carried out. Right: Shape and dimensions of the cage and shielding skirt studied, and the location of sensors.

29 mm, the calculated net solidity ($Sn = 2d/s$) is 0.19. To estimate the velocity flow reduction inside the cage and in its wake the expressions by Løland (1993) and Føre et al. (2020) are used. Løland (1993) proposed a theoretical expression for the non-dimensional velocity reduction factor r behind a net panel based on the solidity (Sn) of the nets: $r = u_w/U_0$ where u_w is the flow velocity in the wake of the cage and U_0 is the free-stream velocity. The velocity reduction factor r is defined as $r = 1 - 0.46C_d$, where C_d is the drag of the netpanel calculated from Sn with the following expression $C_d = 0.04 + (-0.04 + 0.33S_n + 6.54S_n^2 - 4.88S_n^3)$. By performing measurements with net panels with solidity (Sn) ranging from 0.15 to 0.32 Føre et al. (2020) found that an improved expression for r was: $r = 1.02 - 0.84S_n$. In the following the different formulations for the velocity flow reduction are represented together with the measurements data at different location.

3. Results and discussion

3.1. Preprocessing of data

Velocity spikes caused by Doppler noise, signal aliasing and disturbances from the fish as the cage was fully stocked, were removed by filtering the raw data from the ADVs using the improved phase space filter (Goring and Nikora, 2002) for bubbly flows (Birjandi and Bibeau, 2011). Velocity spikes were not replaced, the ADV data were averaged over 1 min and if more than 50% of the data in a minute had been removed, the entire minute was excluded from further analyses.

To establish the characteristic of the flow field around a conical net, a stable incoming current was necessary hence certain critera were set for the incoming current. Previous measurements at the Fornes farm site in accord with NS9415 (Standard Norway, 2009) found that the main current direction was towards North-East (45–60°), and South-West (210–225°), and that the site was influenced by the tidal current. The ADCP and DCP data agreed well with this (see Fig. 2 and Fig. 3). The data from each sensor was therefore averaged over 30 min intervals and if the current direction in the upstream sensor was between 30° and 75° or between 200° and 245°, the sample was categorized as Northward or Southward, respectively.

In addition to these requirements, the standard deviation in the upstream sensor during each 30 min sample could not exceed 30°, the averaged horizontal speed had to be over 0.05 m/s and only dates where there was little to no signs of density stratifications in the water column were considered. The criteria set for the current upstream of the cage are summarised in Table 1.

The current had a clear semi-diurnal tidal pattern (Figs. 2 and 3), with the Nortek ADCPs current direction measurements appearing less structured than the Aanderaa's DCP. This is partially due to the direction fluctuating around 0/360°, but also due to the Aanderaa DCP having a higher temporal resolution and being positioned downstream when the current was moving Southwards making it appear more structured throughout the period (Figs. 2 and 3). The stratification of the water column is evident in Fig. 3 displaying the speed of the Aanderaa's DCP, for instance on the 3rd of July when the top layers had a lower speed than the deeper layers. CTD profiles were also taken irregularly throughout the campaign and showed a clear pycnocline on the 3rd of July at 7.5 m depth that gradually moved up to 3 m depth on the 4th before disappearing on the 5th. CTD data is published in Jónsdóttir et al. (2020). It was therefore only the later periods of the 4th of July and the 5th of July that were relevant for establishing a more or less homogenous current flow field around the conical cage.

The requirements resulted in four data series with the current heading towards the south with a minimum and maximum average direction of 216° and 244°, and seven data series with the current heading towards the north with a minimum and maximum average direction of 32° and 75°. The relevant periods are listed in Table 2.

For the ADVs there was an additional condition for the relevant sampling periods. If more than 16 min of the 30 min averaged over in a period had been removed when using the phase space filter for bubbly flow, the sample was removed from further analysis. This requirement was set to each individual depth, hence some samples have no data from certain depths (see Figs. 4 and 5).

The short duration of this study and the limited number of periods satisfying the criteria should be noted. However, given the depth at Fornes, the clear tidal influence of the site and the farm layout, the results give an clear indication of how the current flow around a conical cage differs from that of a cylindrical cage.

3.2. Current flow during selected periods

The average current speed and direction in all sensors were calculated for the relevant periods listed in Table 2 and are presented in Figs. 4 and 5. The current speed inside the cage at all depths were lower than the speed measured upstream of the cage, but was not necessarily higher than the speed measured downstream of the cage (Figs. 4 and 5).

The maximum average current speed at the inside of the cage was 6 cm/s, while the maximum average current speed outside was 15 cm/s. The current direction inside of the cage did not always agree with the current direction upstream and downstream of the cage. The current downstream and upstream were in relatively good agreement except at 3 m when the current was heading southwards, and a slight disagreement in some of the cases at 3 m and 12 m when heading Northwards. However, this discrepancy could be influenced by the fluctuation around

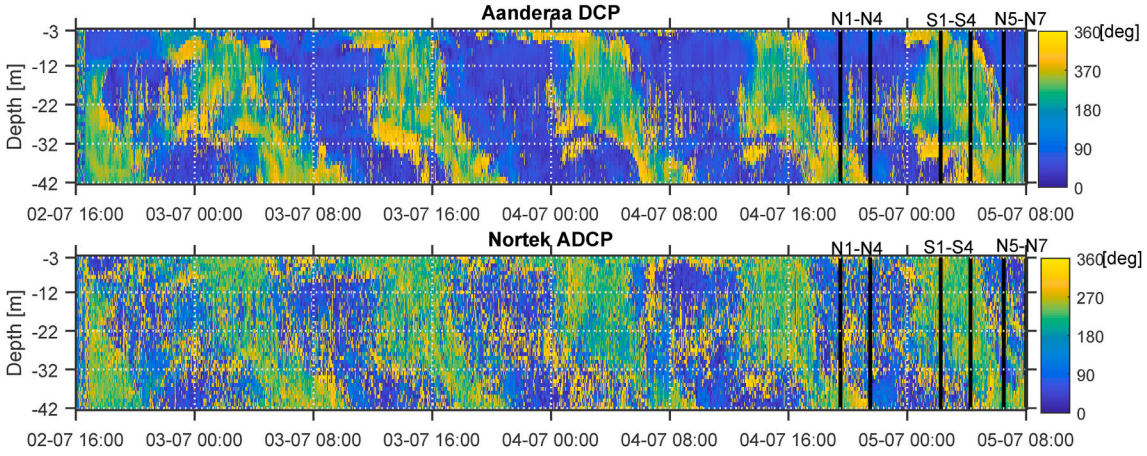

Fig. 2. Current direction recorded by the DCP and ADCP throughout the entire period, respectively. Position of sensors are shown in Fig. 1. Periods described in Table 2 are marked with vertical lines.

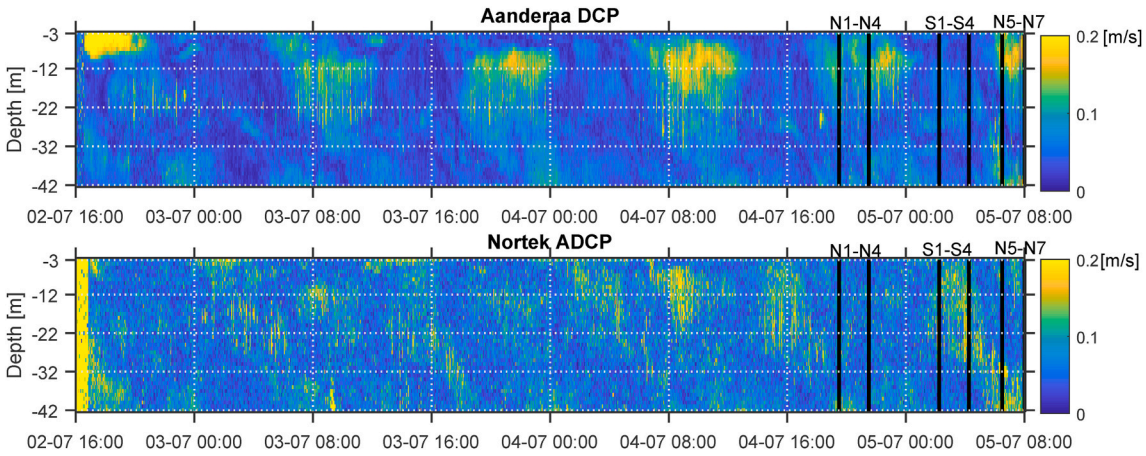

Fig. 3. Horizontal current speed recorded by the DCP and ADCP throughout the entire period, respectively. Position of sensors are shown in Fig. 1. Periods described in Table 2 are marked with vertical lines.

Table 1
Criteria for each 30-min averaged sample current upstream of the cage to be included in further analysis.

	Criteria
Northward	$30° \leq$ direction $\leq 75°$
Southward	$200° \leq$ direction $\leq 245°$
Current speed	> 0.05 m/s
Std. direction	$\leq 30°$

Table 2
Periods where the upstream current has passed the set requirements summarised in Table 1.

Northward		Southward	
Name	Date and Time	Name	Date and Time
N1	04-07-19 19:30–20:00	S1	05-07-19 02:15–02:45
N2	04-07-19 20:00–20:30	S2	05-07-19 02:45–03:15
N3	04-07-19 20:30–21:00	S3	05-07-19 03:15–03:45
N4	04-07-19 21:00–21:30	S4	05-07-19 03:45–04:15
N5	05-07-19 06:30–07:00		
N6	05-07-19 07:00–07:30		
N7	05-07-19 07:30–08:00		

0/360°.

The difference in direction between inside and upstream of the cage could be caused by the recirculation pattern seen in Lien et al. (2014). As this pattern was not observed when fish was present in a shielded cage (Klebert and Su, 2020), it is however more likely that this variation in direction was caused by the very low current speeds inside the cage.

3.3. Flow through cage and net

To compare data from different sensors the characteristic horizontal current speed was established by averaging the horizontal speed in each sensor over all sample periods defined in Table 2 for each depth. To ensure that there were no topographic effects or other effects dependent on the direction of the current, the two groups Northwards and Southwards were preserved. The characteristics horizontal current speed was then normalized using the maximum averaged horizontal current speed recorded upstream independent of depth (Fig. 6).

The results from this study differ from those observed in unshielded cylindrical cages. The current through an unshielded cylindrical cage had a linear reduction from the sensor upstream to the sensor downstream (Klebert et al., 2015). Downstream of the cage there was a reduction in current speed the entire depth of the cage, and below the cage there was an acceleration of the current (Klebert et al., 2015). No such acceleration could be observed in this study due to the spatial limitation of the sensors, but it is unlikely that any such acceleration would have occurred at Fornes due to its conical shape.

In the upper 22 m of the 55 m deep conical cage there was a clear reduction in current speed downstream independently of current direction, similar to that observed for cylindrical cages. Below 22 m however there was no visible blocking effect from the cage (Fig. 6). This is likely due to the tapered shape and smaller diameter of the cage at that depth, which is only 28 m. The reduction in speed downstream was at its highest in the upper 10 m of the cage. This is particularly clear for the current that was heading Southwards, which has an increase in normalized current speed from 9 m depth and deeper. This pattern was not as evident in the downstream current heading Northwards, but the highest reduction rates were still within the top 10 m. These results indicate that the permeable skirt enhanced the reduction of current flow downstream of the cage.

The current flow upstream also appear to be influenced by the skirt with a non-linear response upstream of the skirt volume and a near linear response from 9 m when the current was heading Northward (Fig. 6). The skirt could have influenced the current upstream by decelerating the incoming current flow. As the effect was not constant upstream of the skirt, the slower velocity closer to the surface could have been caused by the stratification at Fornes. The hydrographic conditions at Fornes are detailed in Jónsdóttir et al. (2020), and describe a pycnocline that broke down from the 2nd to the 5th of July. On the 4th of July a weak pycnocline was present at roughly 2 m depth with homogeneous water below, while the water column was homogeneous on the 5th. It was assumed that the pycnocline would have little effect on the characteristic current flow as the normalized current speed was determined by averaging over data from late on 4 th and the 5 th of July. However, given the position of the pycnocline, it is possible that it had some effect on the current speed at 3 m depth.

The increase in current speed downstream of the cage at 9 m when the current was heading southwards could be due to deformations of the skirt. When the current speed is sufficiently high the upstream section of the skirt can creep upwards as it is pushed into the cage, while the downstream section will lift and stand out like a sail (Lien et al., 2014). How the downstream section deforms is dependent on if the skirt is installed as one whole piece or as a long piece of fabric where the ends overlap. At Fornes the skirt was installed as one piece of fabric overlapping at the south side of the cage. At the overlap the skirt was observed to balloon out behind the cage up to several meters at times (Fig. 7). The ballooning in Fig. 7 was probably due to the shorter period of currents close to 20 cm/s just prior to the picture being taken (Fig. 3). A preliminary study at the same site in 2018 observed skirt deformations

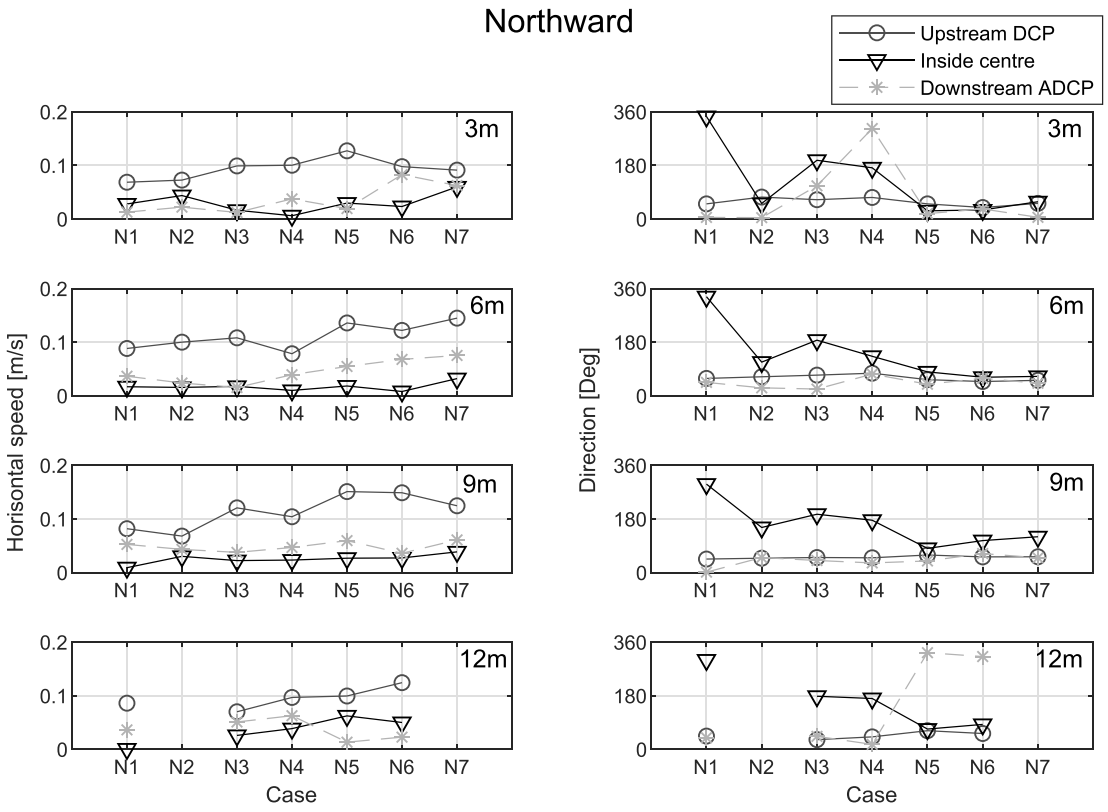

Fig. 4. Horizontal speed and current direction averaged over 30-min for the upstream DCP, downstream ADCP and ADVs inside the cage, for each individual case defined in Table 1 that had a main Northward direction.

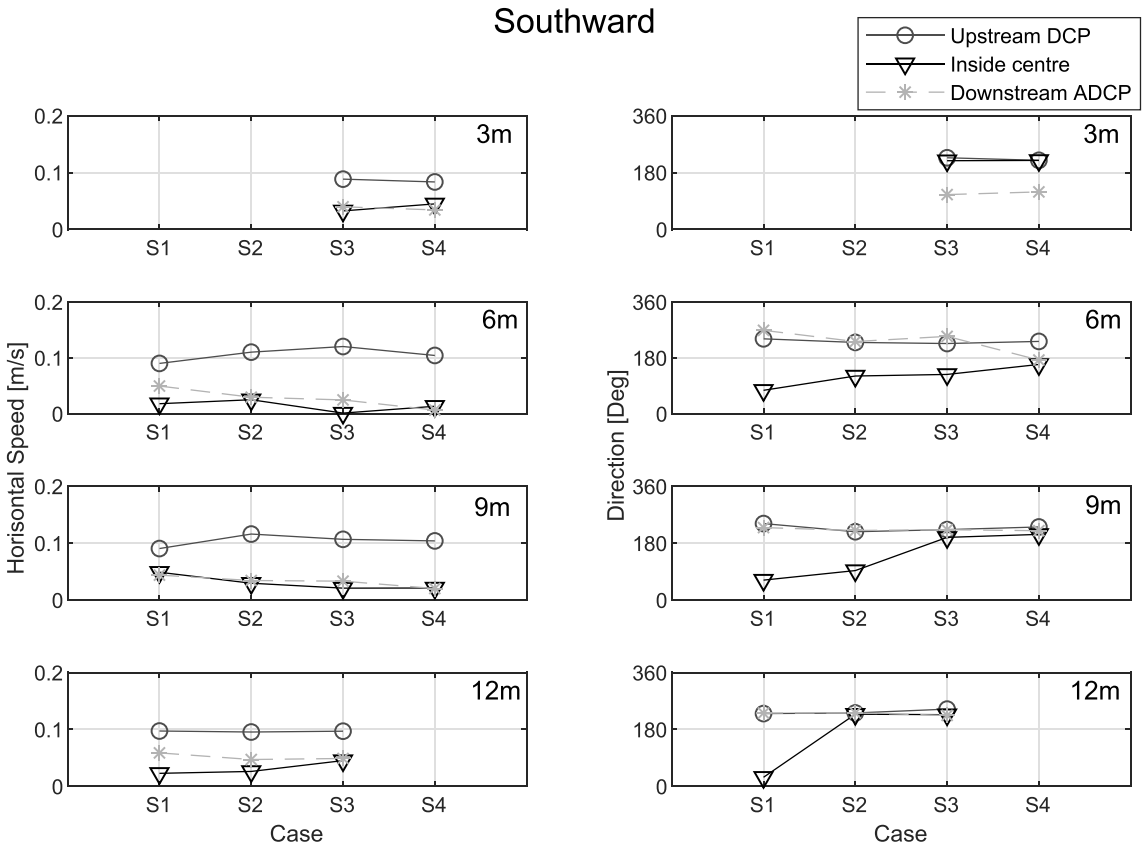

Fig. 5. Horizontal speed and current direction averaged over 30-min for the upstream ADCP, downstream DCP and ADVs inside the cage, for each individual case defined in Table 2 that had a main Southward direction.

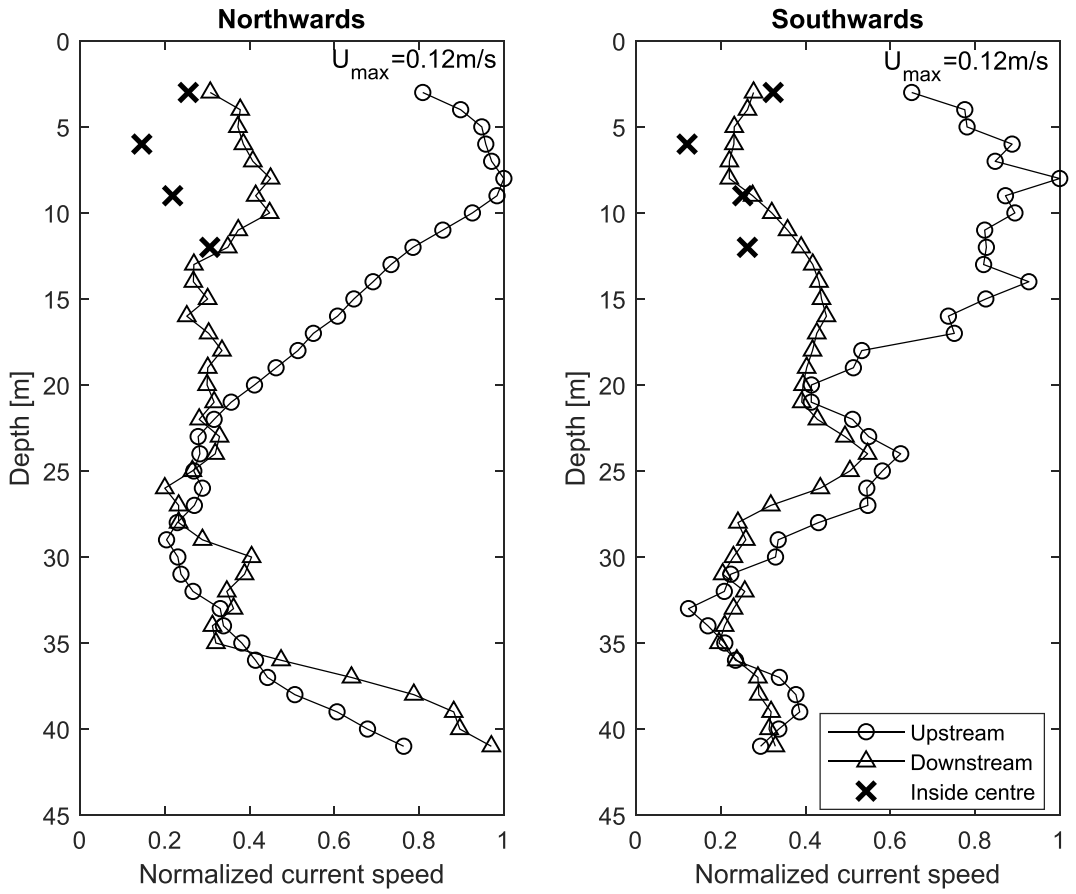

Fig. 6. Average normalized horizontal current speed recorded at each depth in both the upstream, downstream and sensor inside. The maximum average current speed was slightly below 0.12 m/s for both cases.

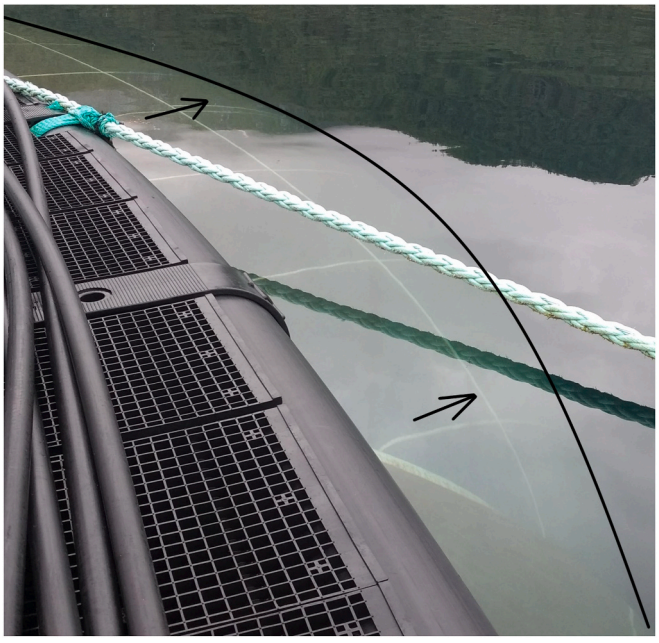

Fig. 7. Black line marks the visible edge of the skirt being lifted due to the current. Black arrows indicate the main current direction (roughly South-West in this image). Image taken the 4th of July at 13:33 local time. The average current upstream (Position A) had a horizontal speed of roughly 8 cm/s at this given time, but had been as high as 20 cm/s only an hour prior, as seen in Fig. 2. The overlap of the skirt is visible just beneath the bottom arrow.

by use of pressure sensors along the bottom of the skirt and registered greater vertical deformation of the skirt downstream than upstream when currents exceeded roughly 13 cm/s (Volent et al., 2020). It should be noted that the horizontal speed inside and downstream of the cage were very low during the selected periods (Figs. 4 and 5) so it's uncertain if the skirt was deforming at all during the chosen periods.

The normalized average current speed on the inside of the cage was lower or equal to the current speed downstream (Fig. 6), thereby not replicating the linear reduction through the cage seen for unshielded cylindrical cages (Klebert et al., 2015). The current speed inside the cage followed a similar pattern independent of current directions with a strong average current speed at 3 m depth, the weakest current speed at 6 m depth, and an increase in current speed from 6 to 12 m depth (Fig. 6). It should also be noted that there were only two samples included in the Southward data group at 3 m depth (see Fig. 5), which could explain why the normalized current speed was at its highest inside the cage at 3 m depth when the current was heading Southwards.

The high reduction at 6 m depth could be due to the vertical positioning of the biomass in the cage as biomass can increase the reduction in speed (Klebert and Su, 2020). During this study the stocking density was 19 kg m^{-3}. Atlantic salmon rarely distributes themselves evenly vertically in the cage and prefer to swim at deeper depths during the day and closer to the surface during night (Oppedal et al., 2011). As this study took place during the summer in Northern Norway the sun never set, and the continuous daylight may have resulted in the salmon swimming in a higher density at 6 m and below, thereby reducing the current speed there more than other layers. Unfortunately, the behaviour of the salmon was not monitored during this study.

3.4. Reduction in current speed

The reduction factor (r) was calculated for 3, 6, 9 and 12 m and compared with the reduction factor found using the expressions by Løland (1993) and Føre et al. (2020) (Fig. 8). The expression by Føre et al. (2020) was better at estimating the current reduction downstream of the skirt (Sn = 0.51) than Løland (1993). This was expected as the expression by Føre et al. (2020) is developed to correctly estimate the current downstream of nets with high solidity.

The reduction from upstream to inside the cage was however higher than expected compared with both expressions. This could be due to the low current speed in this study as the lowest incoming current speed utilised in Føre et al. (2020) was 0.25 m/s, compared to 0.05 m/s in this study. Furthermore, both Løland (1993) and Føre et al. (2020) utilised

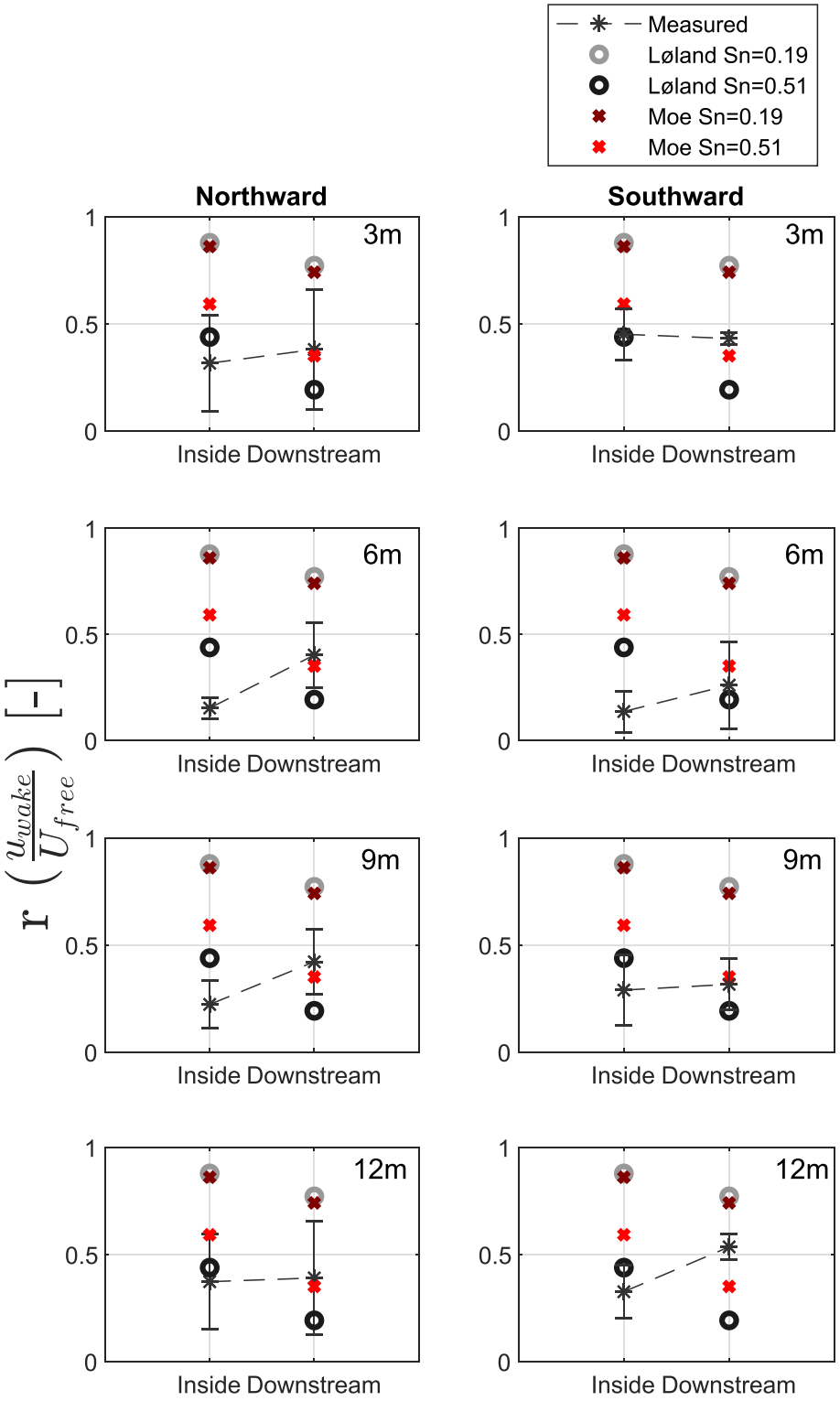

Fig. 8. Average reduction ratio (r) between current speed inside and upstream, and downstream and upstream, measured in this study. Expected reduction ratio behind one net panel and two net panels using Løland (1993) and Føre et al. (2020) are also marked using Sn = 0.19 and Sn = 0.51.

stretched out plane nets. The conical cage in this study had an inclination angle, which would have increased the reduction, but also had the opportunity to deform. There could also have been biofouling on both the net and skirt, which would have increased the solidity and reduction in current speed through the cage. As the estimate by Føre et al. (2020) was good downstream of the cage, but not inside the cage, it could be that the biomass around the ADVs resulted in low current speeds. Another reason is that comparing ADV data with ADCP data is not optimal, as the ADV averages over a very small volume while the ADCP averages over cell sizes of 1 m.

The highest reduction inside the cage was 86% ($r = 0.14$) at 6 m depth. For unshielded cages exposed to currents as strong as 60 cm/s the reduction from outside to inside is 21.5% at 6 m depth (Klebert et al., 2015). In another study by Johansson et al. (2014) the reduction inside a non-shielded cage varied from 0 to 50% when the speed outside was 20 cm/s (Johansson et al., 2014). Given the high biomass in this study, inclination of the cage, the general low current speeds during the relevant periods and the presence of a shielding skirt, a reduction of 86% was deemed reasonable.

4. Conclusion

Current speed upstream, downstream and inside a conical full-scale shielded sea cage were monitored. The velocity measurement inside the cage showed a more complex flow pattern than for a cylindrical cage, probably due to the interaction between the permeable skirt and the conical shape of the cage which could both have affected the distribution of fish in the water column differently than in a cylindrical cage. Speed was generally low inside the cage. The weakest current speed inside the cage was at 6 m depth independently of direction. Current speed increased beneath this depth. There was a clear reduction in current speed downstream of the shielding skirt, with the highest reduction recorded behind the shielded volume. No blocking effect was observed beneath 22 m depth, probably due to the conical shape of the cage. The difference in current flow field behind the conical cage compared with a cylindrical cage may have implications for the dispersal of waste, feed pellets and microorganisms from the cage influencing the benthic impact of the farm, and further work should focus on documenting these differences.

CRediT authorship contribution statement

Kristbjörg Edda Jónsdóttir: Conceptualization, Data curation, Methodology, Visualization, Writing - original draft. **Pascal Klebert:** Conceptualization, Writing - original draft. **Zsolt Volent:** Conceptualization, Data curation, Funding acquisition, Visualization, Writing - original draft. **Jo Arve Alfredsen:** Writing - review & editing.

Declaration of competing interest

The authors declare that they have no known competing financial interests or personal relationships that could have appeared to influence the work reported in this paper.

Acknowledgement

This study is part of the project “Shielding skirt as a method for prevention and control of salmon lice infestation – improving knowledge about environmental conditions for increase in efficiency and reduction of risk (SKJERMTEK)” (project number: 901396) funded by The Norwegian Seafood Research Fund (FHF). KEJ received funding from the RACE research grant program funded by SINTEF Ocean. We are thankful for access to equipment from SINTEF ACE, and to Nordlaks Oppdrett AS for access to their sites and the help received from their on-site employees.

References

Abolofia, J., Asche, F., Wilen, J.E., 2017. The cost of lice: quantifying the impacts of parasitic sea lice on farmed salmon. Mar. Resour. Econ. 32, 329–349.

Bi, C.W., Zhao, Y.P., Dong, G.H., Xu, T.J., Gui, F.K., 2013. Experimental investigation of the reduction in flow velocity downstream from a fishing net. Aquacult. Eng. 57, 71–81. https://doi.org/10.1016/j.aquaeng.2013.08.002. http://www.sciencedirect.com/science/article/pii/S0144860913000691.

Bi, C.W., Zhao, Y.P., Dong, G.H., Zheng, Y.N., Gui, F.K., 2014. A numerical analysis on the hydrodynamic characteristics of net cages using coupled fluid–structure interaction model. Aquacult. Eng. 59, 1–12.

Birjandi, A.H., Bibeau, E.L., 2011. Improvement of acoustic Doppler velocimetry in bubbly flow measurements as applied to river characterization for kinetic turbines. Int. J. Multiphas. Flow 37, 919–929.

Bui, S., Stien, L.H., Nilsson, J., Trengereid, H., Oppedal, F., 2020. Efficiency and welfare impact of long-term simultaneous in situ management strategies for salmon louse reduction in commercial sea cages. Aquaculture 520, 734934.

Føre, H.M., Endresen, P.C., Norvik, C., Lader, P.F., 2020. Hydrodynamic loads on net panels with different solidities. In: Proceedings of 39th International Conference on Ocean, Offshore and Arctic Engineering (OMAE). ASME.

Frank, K., Gansel, L., Lien, A., Birkevold, J., 2015. Effects of a shielding skirt for prevention of sea lice on the flow past stocked salmon fish cages. J. Offshore Mech. Arctic Eng. 137.

Fredheim, A., 2005. Current Forces on Net Structure. Phd Thesis. Norwegian University of Science and Technology.

Gansel, L.C., Rackebrandt, S., Oppedal, F., McClimans, T.A., 2014. Flow fields inside stocked fish cages and the near environment. J. Offshore Mech. Arctic Eng. 136, 31201. https://doi.org/10.1115/1.4027746, 031201.

Gansel, L.C., Plew, D.R., Endresen, P.C., Olsen, A.I., Misimi, E., Guenther, J., Jensen, Ø., 2015. Drag of clean and fouled net panels–measurements and parameterization of fouling. PloS One 10, e0131051.

Geitung, L., Oppedal, F., Stien, L.H., Dempster, T., Karlsbakk, E., Nola, V., Wright, D.W., 2019. Snorkel sea-cage technology decreases salmon louse infestation by 75% in a full-cycle commercial test. Int. J. Parasitol. 49, 843–846.

Goring, D.G., Nikora, V.I., 2002. Despiking acoustic Doppler velocimeter data. J. Hydraul. Eng. 128, 117–126.

Heuch, P.A., Parsons, A., Boxaspen, K., 1995. Diel vertical migration: a possible host-finding mechanism in salmon louse (lepeophtheirus salmonis) copepodids? Can. J. Fish. Aquat. Sci. 52, 681–689.

Hevrøy, E., Boxaspen, K., Oppedal, F., Taranger, G., Holm, J., 2003. The effect of artificial light treatment and depth on the infestation of the sea louse lepeophtheirus salmonis on atlantic salmon (salmo salar l.) culture. Aquaculture 220, 1–14.

Huse, I., Holm, J., 1993. Vertical distribution of atlantic salmon (salmo salar) as a function of illumination. J. Fish. Biol. 43, 147–156.

Iversen, A., Hermansen, Ø., Nystøyl, R., Hess, E.J., 2017. Kostnadsutvikling I Lakseoppdrett–Med Fokus På Fã'r-Og Lusekostnader. Nofima rapportserie.

Johansson, D., Juell, J.E., Oppedal, F., Stiansen, J.E., Ruohonen, K., 2007. The influence of the pycnocline and cage resistance on current flow, oxygen flux and swimming behaviour of atlantic salmon (salmo salar l.) in production cages. Aquaculture 265, 271–287.

Johansson, D., Laursen, F., Fernö, A., Fosseidengen, J.E., Klebert, P., Stien, L.H., Vågseth, T., Oppedal, F., 2014. The interaction between water currents and salmon swimming behaviour in sea cages. PloS One 9, e97635.

Jónsdóttir, K.E., Volent, Z., Alfredsen, J.A., 2020. Dynamics of dissolved oxygen inside salmon sea-cages with lice shielding skirts at two hydrographically different sites. Aquacult. Environ. Interact. 12, 559–570. https://doi.org/10.3354/aei00384.

Kim, T., Lee, J., Fredriksson, D.W., DeCew, J., Drach, A., Moon, K., 2014. Engineering analysis of a submersible abalone aquaculture cage system for deployment in exposed marine environments. Aquacult. Eng. 63, 72–88.

Klebert, P., Su, B., 2020. Turbulence and flow field alterations inside a fish sea cage and its wake. Appl. Ocean Res. 98, 102113.

Klebert, P., Lader, P., Gansel, L., Oppedal, F., 2013. Hydrodynamic interactions on net panel and aquaculture fish cages: a review. Ocean Eng. 58, 260–274.

Klebert, P., Patursson, Ø., Endresen, P.C., Rundtop, P., Birkevold, J., Rasmussen, H.W., 2015. Three-dimensional deformation of a large circular flexible sea cage in high currents: field experiment and modeling. Ocean Eng. 104, 511–520. https://doi.org/10.1016/j.oceaneng.2015.04.045. http://www.sciencedirect.com/science/article/pii/S0029801815001262.

Kristiansen, T., Faltinsen, O.M., 2015. Experimental and numerical study of an aquaculture net cage with floater in waves and current. J. Fluid Struct. 54, 1–26.

Lader, P., Dempster, T., Fredheim, A., Jensen, Ø., 2008. Current induced net deformations in full-scale sea-cages for atlantic salmon (salmo salar). Aquacult. Eng. 38, 52–65. https://doi.org/10.1016/j.aquaeng.2007.11.001. http://www.sciencedirect.com/science/article/pii/S0144860907000957.

Lee, C.W., Kim, Y.B., Lee, G.H., Choe, M.Y., Lee, M.K., Koo, K.Y., 2008. Dynamic simulation of a fish cage system subjected to currents and waves. Ocean Eng. 35, 1521–1532.

Lien, A.M., Volent, Z., Jensen, Ø., Lader, P., Sunde, L.M., 2014. Shielding skirt for prevention of salmon lice (lepeophtheirus salmonis) infestation on atlantic salmon (salmo salar l.) in cages–a scaled model experimental study on net and skirt deformation, total mooring load, and currents. Aquacult. Eng. 58, 1–10.

Løland, G., 1993. Current forces on, and water flow through and around, floating fish farms. Aquacult. Int. 1, 72–89.

Mayer, D.A., Virmani, J.I., Weisberg, R.H., 2007. Velocity comparisons from upward and downward acoustic Doppler current profilers on the west Florida shelf. J. Atmos. Ocean. Technol. 24, 1950–1960.

Norway, Standard, 2009. Marine Fish Farms-Requirements for Site Survey, Risk Analyses, Design, Dimensioning, Production, Installation and Operation. norsk standard ns 9415. E, Norway.
Oppedal, F., Dempster, T., Stien, L.H., 2011. Environmental drivers of atlantic salmon behaviour in sea-cages: a review. Aquaculture 311, 1–18.
Oppedal, F., Samsing, F., Dempster, T., Wright, D.W., Bui, S., Stien, L.H., 2017. Sea lice infestation levels decrease with deeper 'snorkel'barriers in atlantic salmon sea-cages. Pest Manag. Sci. 73, 1935–1943.
Patursson, Ø., 2008. Flow through and Around Fish Farming Nets. Ph.D. thesis. Ocean Engineering, University of New Hampshire, Durham, NH03824, USA.
Rasmussen, H.W., Patursson, Ø., Simonsen, K., 2015. Visualisation of the wake behind fish farming sea cages. Aquacult. Eng. 64, 25–31.
Remen, M., Aas, T.S., Vågseth, T., Torgersen, T., Olsen, R.E., Imsland, A., Oppedal, F., 2014. Production performance of atlantic salmon (salmo salar l.) postsmolts in cyclic hypoxia, and following compensatory growth. Aquacult. Res. 45, 1355–1366.
Stien, L.H., Nilsson, J., Hevrøy, E.M., Oppedal, F., Kristiansen, T.S., Lien, A.M., Folkedal, O., 2012. Skirt around a salmon sea cage to reduce infestation of salmon lice resulted in low oxygen levels. Aquacult. Eng. 51, 21–25.
Stien, L.H., Lind, M.B., Oppedal, F., Wright, D.W., Seternes, T., 2018. Skirts on salmon production cages reduced salmon lice infestations without affecting fish welfare. Aquaculture 490, 281–287.
Volent, Z., Jónsdóttir, K.E., Misund, A., Steinhovden, K.B., Chauton, M.S., Sunde, L.M., 2020. Strategi Lakselus 2017: Luseskjørt Som Ikke-Medikamentell Metode for Forebygging Og Kontroll Av Lakselus – Utvikling Av Kunnskap Om Miljøforhold for Økt Effekt Og Redusert Risiko (SKJERMTEK). SINTEF Ocean. Report 302003409.
Zhao, Y.P., Bi, C.W., Chen, C.P., Li, Y.C., Dong, G.H., 2015. Experimental study on flow velocity and mooring loads for multiple net cages in steady current. Aquacult. Eng. 67, 24–31.